

# Year-round high abundances of the world's smallest marine vertebrate (*Schindleria*) in the Red Sea and worldwide associations with lunar phases

Vanessa Robitzch (✉ [Vanessa.robitzchsierra@kaust.edu.sa](mailto:Vanessa.robitzchsierra@kaust.edu.sa))

Austral University of Chile

Victor Molina-Valdivia

University of Valparaíso

Jaiber Solano-Iguaran

Austral University of Chile

Mauricio Landaeta

University of Valparaíso

Michael Lee Berumen

King Abdullah University of Science and Technology

---

## Research Article

**Keywords:** coral reef fish, reproduction, light traps, otoliths, pedomorphism, Saudi Arabia

**Posted Date:** March 19th, 2021

**DOI:** <https://doi.org/10.21203/rs.3.rs-267432/v1>

**License:**  This work is licensed under a Creative Commons Attribution 4.0 International License.

[Read Full License](#)

---

**Version of Record:** A version of this preprint was published at Scientific Reports on July 12th, 2021. See the published version at <https://doi.org/10.1038/s41598-021-93800-w>.

1 **Title: Year-round high abundances of the world's smallest marine vertebrate**  
2 **(*Schindleria*) in the Red Sea and worldwide associations with lunar phases**

3

4 Vanessa Robitzch<sup>1,2,\*</sup>, Victor Molina-Valdivia<sup>3</sup>, Jaiber J. Solano-Iguaran<sup>2,4</sup>, Mauricio  
5 Landaeta<sup>3,5</sup>, & Michael L. Berumen<sup>1</sup>

6

7 *<sup>1</sup>Red Sea Research Center, Division of Biological and Environmental Science and Engineering,*  
8 *King Abdullah University of Science and Technology, Thuwal, 23955, Saudi Arabia; <sup>2</sup>Instituto*  
9 *de Ciencias Ambientales y Evolutivas, Facultad de Ciencias, Universidad Austral de Chile,*  
10 *Casilla 567, Valdivia, Chile; <sup>3</sup>Laboratorio de Ictioplancton (LABITI), Instituto de Biología,*  
11 *Facultad de Ciencias, Universidad de Valparaíso, Valparaíso, Chile; <sup>4</sup>Departamento de Salud*  
12 *Hidrobiológica, Instituto de Fomento Pesquero, Puerto Montt, Chile; <sup>5</sup>Centro de Observación*  
13 *Marino para Estudios de Riesgos del Ambiente Costero (COSTA-R), Universidad de*  
14 *Valparaíso, Viña del Mar, Chile*

15

16 **\*Correspondence:** Vanessa Robitzch, Instituto de Ciencias Ambientales y Evolutivas,  
17 Universidad Austral de Chile, Campus Isla Teja, Casilla 567, Valdivia, Chile **E-mail:**  
18 Vanessa.RobitzchSierra@kaust.edu.sa

19

20 **Keywords:** coral reef fish, reproduction, light traps, otoliths, paedomorphism, Saudi Arabia

21

22 **Acknowledgments:** For logistic and fieldwork support, we thank the Coastal and Marine  
23 Resources Core Laboratory at the King Abdullah University of Science and Technology  
24 (KAUST), as well as additional fieldwork volunteers. For help with otolith readings, we  
25 particularly thank Camilo Rodríguez-Valentino from the Laboratorio de Esclero-Cronología,

26 Pontificia Universidad Católica de Valparaíso, Chile. This research was supported by KAUST  
27 baseline research funds to MLB and Xabier Irigoyen, and by the 2019 FONDECYT-CONICYT  
28 Postdoctoral fellowship N° 3190891 awarded to VR. This work is dedicated to the late J. E.  
29 Randall, who encouraged VR's fascination for *Schindleria* when her first Red Sea specimens  
30 were identified.

31

## 32 **Abstract**

33 Very little is known about the ecology and biology of the smallest marine vertebrates, fishes in  
34 the genus *Schindleria*. Even though over half of named *Schindleria* species have been described  
35 from the Red Sea, very few specimens have been identified. Here, we assessed abundance  
36 patterns of nearly two thousand Red Sea adults and found evidence for putative seasonal and  
37 spatial differences, likely related to differing habitat and environmental conditions. Within the  
38 Red Sea, the highest abundances were neither found during seasonal temperature extremes nor  
39 during peaks of coral reef fish recruitment. We also found evidence for global trends in  
40 abundances related to lunar cycles, for which data from a recently published large collection of  
41 specimens from the DANA Expedition (1928-1930) were included. The abundance of  
42 *Schindleria* in relation to lunar phases differed significantly, with most *Schindleria* being  
43 caught outside the full moon. Adult specimens in our Red Sea collections were most abundant  
44 during the new moon, while the 3<sup>rd</sup> quarter moon yielded the highest abundances in the DANA  
45 collection. We further suggest that the abundances of *Schindleria* at coral reefs may be related  
46 to reproductive cycles and that these cycles may be timed with the moon, since back-  
47 calculations of hatch dates from otoliths resulted significantly around the new moon.  
48 *Schindleria* may be the most numerous coral reef fish in the world, for which we encourage  
49 increased research.

50

## 51 **Introduction**

52 Schindleriidae is a small cryptic gobioid family, currently comprising only one described genus:  
53 *Schindleria*. These are the smallest vertebrates of the marine realm and the youngest  
54 reproducing vertebrates on the planet<sup>1</sup>. Due to their cryptic biology and the fact that, to our  
55 knowledge, apart from one photograph of an aggregation in the Hawaiian Islands taken by J. E.  
56 Randall documenting their residence over sand and rubble substrata during daytime<sup>2</sup>, they have  
57 never been sighted in their natural habitat elsewhere, nor has it been possible to maintain them  
58 in aquaria<sup>3</sup>. Hence, very little is known about their biology, ecology, and exact distribution.  
59 Furthermore, since adult *Schindleria* are very small in size and have pedomorphic features  
60 (i.e., never undergoing metamorphosis and retaining a larval phenotype throughout their life<sup>4</sup>),  
61 specimens are generally overlooked; and most studies are based on very few samples or report  
62 the sighting of some of these individuals as bycatch of other research purposes, mainly from  
63 light traps and planktonic tows<sup>5,6</sup>. More recent sampling efforts<sup>3,7</sup> and the inspection of museum  
64 collections from plankton tows for the presence of *Schindleria*<sup>8</sup> have increased knowledge and  
65 attention on the presence and distribution of this genus, and high numbers of these fishes have  
66 more recently been studied. Ahnelt and Sauberer (2020) provide a complete overview of all  
67 currently published *Schindleria* sightings and the data available on its distribution<sup>8</sup>. Apart from  
68 the Caribbean and the tropical Atlantic, the family seems to be common across coral reefs  
69 worldwide.

70 *Schindleria* can be found throughout the Indo-Pacific<sup>7-9</sup> and are believed to be “lagoon-  
71 completers”, remaining for their entire lifecycle in shallow coral reef lagoons<sup>10,11</sup>. However,  
72 some specimens have also been collected in coastal waters around volcanic islands with no  
73 lagoons (e.g., Easter Island<sup>5</sup>) as well as relatively distant from coral reefs and at depths of  
74 hundreds of meters<sup>8,9,12-14</sup>; but whether these findings are exceptions or strayed specimens,

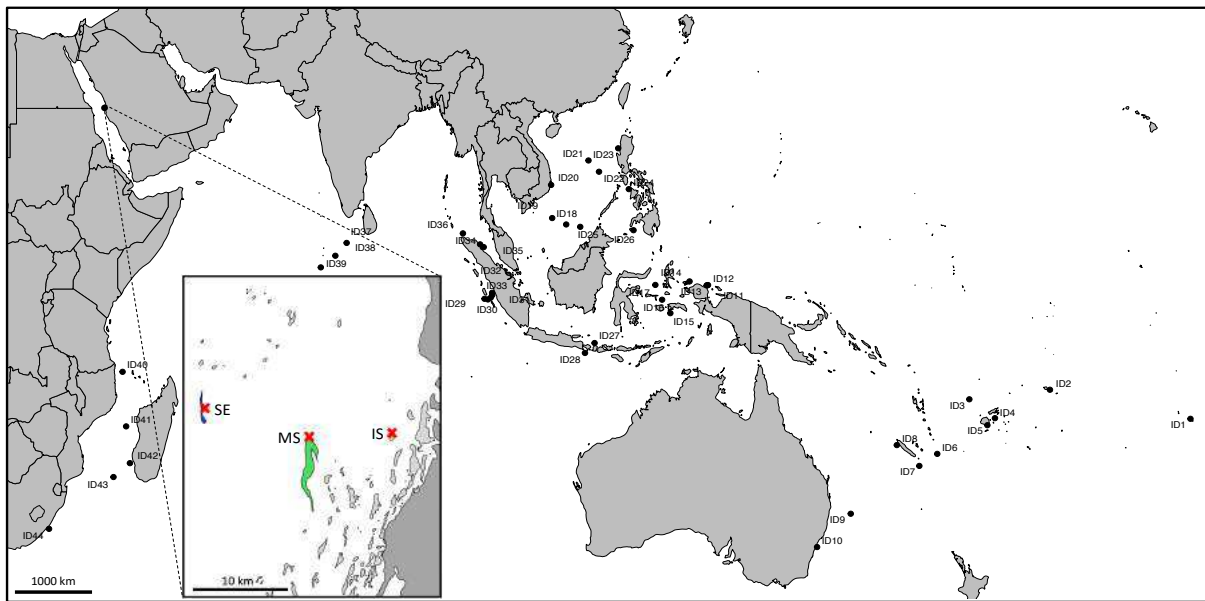
75 individuals advected by strong currents, or whether deeper oceanic environments are also part  
76 of *Schindleria*'s habitat, still remains unanswered and highlights the need for more targeted and  
77 comprehensive sampling efforts. Data about their ecology and biology are also not available  
78 since no study reports observations of specimens in their natural habitat, which remains  
79 speculative. Some authors suggest that *Schindleria* may live in burrows in the sandy bottoms  
80 of the coral reef matrix<sup>10</sup> of which they come out at night, probably to feed and avoid visual  
81 predators. Many studies suggest that they retain a planktonic life (since they were mainly  
82 collected in plankton tows in the pelagic or neritic habitats<sup>15-17</sup> but are in close association with  
83 the reefs<sup>6,7,11</sup>), while Randall and Cea reported daytime aggregations over sand and rubble  
84 substrata in Hawaii<sup>2</sup>, but whether this is a common behavior or aggregations are seasonally  
85 induced, still remains unknown.

86 To date, very few *Schindleria* species have been described. From the seven named species, four  
87 have been described from the Red Sea and only a handful of specimens were collected for the  
88 description of each of these Red Sea species<sup>6,14,18-21</sup>. Genetically, more than 40 different  
89 haplotypes have been identified in the eastern Indo-Pacific based on sequence data from the  
90 16S mitochondrial rDNA gene region, suggesting that there may be a much higher number of  
91 species within the genus<sup>3,7</sup>. Morphologically, it has been very difficult to classify specimens or  
92 discriminate among haplotypes due to the lack of evident characteristic features. As a result,  
93 classification into two main types remains the most commonly used approach<sup>8,22</sup>: a long dorsal  
94 fin type (LDF; with the origin of the dorsal-fin anterior to the origin of the anal fin, by a  
95 minimum of six fin rays), which is also the most commonly sighted<sup>8</sup>; and a short dorsal fin type  
96 (SDF; with the origins of anal and dorsal fin more or less vertically aligned), which seems more  
97 rare and potentially comprises endemic species.

98 Our study assessed the abundance of adult LDF type specimens of *Schindleria* at three reefs  
99 along a cross-shelf environmental gradient in the central Red Sea of Saudi Arabia. We collected  
100 specimens at night, using LED light traps around the new moon of twelve consecutive months  
101 to measure potential changes related to spatio-temporal variations in abundances of *Schindleria*  
102 and assess during which season individuals may be more likely to surface and/or to be present  
103 in the shallow water column of the reefs' matrices. We further hypothesized that mature  
104 *Schindleria* specimens may be coming out of their putative diurnal hideaways and surface at  
105 night<sup>6,11</sup> forming aggregations to reproduce and should thus be more abundant in the catches  
106 around the new moon or darker moon phases, during which their translucent bodies are less  
107 likely to be visible to nocturnal predators. Many marine species show reproductive cycles linked  
108 to lunar patterns<sup>23</sup>. For this purpose, we also collected specimens at the same sites using the  
109 same light traps every day for an entire lunar month to assess whether or not specimens were  
110 rather absent in the catches around the full moon. Lastly, we used the recently published  
111 information on the presence of *Schindleria* in the plankton tows collections from the DANA  
112 Expedition 1928-1930<sup>8</sup> and assessed whether or not abundances of *Schindleria* related to lunar  
113 phases is a global trend. To further support putative links between the biology/reproduction of  
114 *Schindleria* and lunar cycles, we assessed the ages of the mature *Schindleria* specimens from  
115 the Red Sea using daily growth increments of their sagittal otoliths, inferred their hatch dates,  
116 and estimated the length of a putative reproductive cycle of this premature and extremely short-  
117 lived species. To our knowledge, our study is the first based on a collection of nearly two  
118 thousand specimens of *Schindleria* and provides first baseline information on putative temporal  
119 distribution patterns worldwide, as well as year-round abundances in the Red Sea.

120

## 121 **Results**

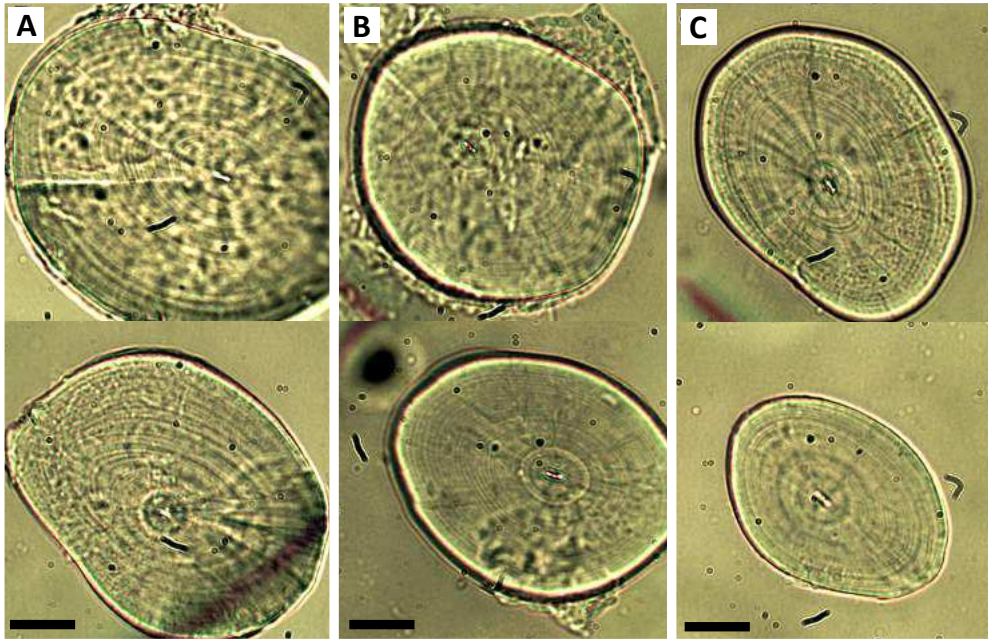


123

124 **Fig. 1:** Collection sites of *Schindleria*: from the DANA Expedition 1928-1930 (all sites  
 125 represented by a “dot”: ID1 – ID44, following Ahnelt and Sauberer 2020<sup>8</sup>); and from the Red  
 126 Sea, with a zoomed-in section displaying the three reefs where collection took place using a  
 127 LED powered light trap along a cross-shelf gradient from the shore to the shelf edge, near the  
 128 coast of Thuwal, Saudi Arabia. Coral reefs within the zoomed-in Red Sea section are given in  
 129 “light grey” while the land sections are in “dark grey” and the sampled reef sites are color  
 130 coded, with the “yellow” reef inshore (IS), the “green” reef at the mid-shelf (MS), and the  
 131 “blue” reef at the shelf edge (SE). The “red” crosses indicate the location of deployment of the  
 132 LED powered light traps for this study.

133

134 A total of 1996 adult *Schindleria* specimens were collected for this study using LED light traps  
 135 in the central Red Sea, Thuwal, Saudi Arabia (Fig. 1). From these, 44 specimens were selected  
 136 for the extraction of otoliths, out of which 41 specimens were successfully aged by reading the  
 137 number of daily growth increments of at least one sagittal otolith in order to assess lunar  
 138 reproductive cycles (Fig. 2).



139

140 **Fig. 2:** Sagittal otoliths from mature *Schindleria* specimens sampled with light traps from an  
 141 inshore (A), a mid-shelf (B), and a shelf-edge (C) reef in the Red Sea, near the coast of Thuwal,  
 142 Saudi Arabia. These otoliths represent otoliths of ideal conditions (i.e., “C3” category) to count  
 143 daily growth increments and yielded average numbers of increments (between 30-33) despite  
 144 slightly differing shapes and sizes. All otoliths are to scaled, with the bar at the bottom (left) of  
 145 each panel representing 20  $\mu\text{m}$ . The otolith at the top of each panel represents a rounder and  
 146 larger otolith while the otolith at the bottom a more oval-shaped and smaller otolith.

147

148 For the assessment of abundances in relation to moon phases, 204 specimens were collected  
 149 during the daily sampling efforts within a lunar month (from the 16<sup>th</sup> October to the 16<sup>th</sup>  
 150 November, 2014). For the yearlong spatio-temporal assessment of abundances in the Red Sea,  
 151 a total of 1792 specimens were caught from February 2015 to January 2016.

152 Additionally, data on the temporal abundance of 502 specimens from the DANA Expedition  
 153 were used to assess putative worldwide trends in abundances of *Schindleria* with moon phases  
 154 (Table 1).

155

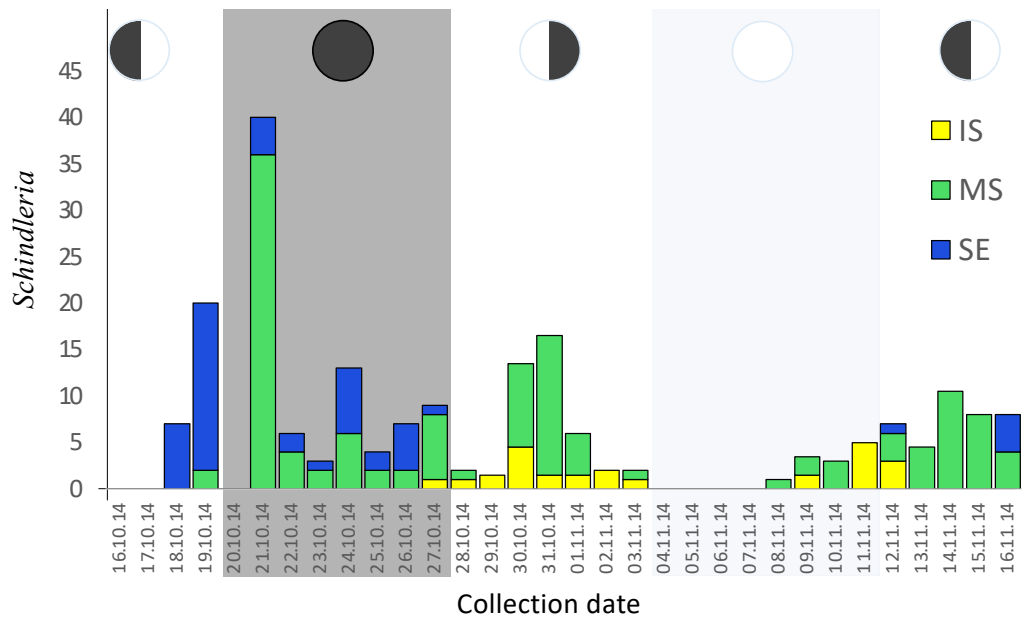
156 **Table 1:** Total abundances of *Schindleria* (All) observed in each of the four main moon  
157 phases: the new moon (NM), the 1<sup>st</sup> quarter moon (1stQ), the full moon (FM), and the 3<sup>rd</sup> quarter  
158 moon (3rdQ) comprising two different data sets: The Red Sea collections (at an inshore (IS:  
159 22.3055 °N, 39.0493 °E), a mid-shelf (MS: 22.3054 °N, 38.9684 °E), and a shelf-edge (SE:  
160 22.3415 °N, 38.8538 °E) reef) and the collection from the DANA Expedition from 1928-1930  
161 (DANA).

Collection	Moon Phase			
	<i>NM</i>	<i>1stQ</i>	<i>FM</i>	<i>3rdQ</i>
<b>All</b>	200	139	35	332
<b>DANA</b>	116	97	15	274
<b>Red Sea</b>	84	42	20	58
<i>Inshore</i> (IS)	2	12	10	0
<i>Mid-shelf</i> (MS)	60	30	9	29
<i>Shelf-edge</i> (SE)	22	0	1	29

162

163 *Abundances of Schindleria related to lunar phases*

164 Out of the 204 specimens collected daily during a lunar month (Oct-Nov, 2014) in the Red Sea,  
165 only 4 % were caught during the days around the full moon ( $\pm 3$  days), while more than 40 %  
166 were caught during the days around the new moon ( $\pm 3$  days) (see Fig. 3). Similarly, during the  
167 DANA Expedition, only 3 % of the 502 *Schindleria* specimens were caught during days around  
168 the full moon ( $\pm 3$  days), while more than 33 % were caught during days around the new moon  
169 ( $\pm 3$  days). In both cases there was a tenfold increase in *Schindleria* from full moon to new moon  
170 catches (Table 1).



171

172 **Fig. 3:** Barplot representing the total abundances of *Schindleria* collected during one lunar cycle

173 in the Red Sea of Saudi Arabia. Total numbers of *Schindleria* specimens (y-axis) collected are

174 color-coded for the relative number caught at each of three sampling locations: an inshore reef

175 (IS) in “yellow”, a reef at the mid-shelf (MS) in “green”, and one at the shelf-edge (SE) in

176 “blue”. Collections took place using three replicate LED powered light traps (collapsible

177 Bellamare model) at each sampling location for the period of 32 consecutive nights from the

178 16<sup>th</sup> October to the 16<sup>th</sup> November (2014; x-axis). Different moon phases are indicated with pie

179 charts on the top of each shaded section of the plot starting with the 3<sup>rd</sup> quarter moon, followed

180 by the new moon, the 1<sup>st</sup> quarter moon, the full moon, and ending again with the 3<sup>rd</sup> quarter

181 moon (from left to right).

182

183 Otolith counts revealed the median age of mature *Schindleria* specimens from the Red Sea to

184 be 33 days ( $\pm 3$  days; Table 2, Fig. 2). Moreover, through the back-calculation of the hatch

185 dates using the age of the specimens and the collection date, we found a significant hatch pattern

186 with lunar periodicity (Rao’s spacing test,  $P < 0.01$ ), for which the angular mean was found a

187 few days after the new moon (Fig. 4). Together, the abundances of adult *Schindleria* and the

188 derived hatching events indicated that *Schindleria* may be approaching the reef around the new  
 189 moon for reproduction after which a couple of days later the eggs hatch, the larvae grow, and  
 190 the specimens mature to return to the reef matrix for reproduction on time for the next new  
 191 moon, from which their reproductive cycle starts over. The oldest two individuals in our sample  
 192 were 44 and 42 days old; all others were less than 40 days old. Females carried large eggs and  
 193 their ovaries were relatively full. Males had well developed urogenital papillae and all  
 194 specimens had similar body lengths, within the expected size range of adults. It thus seems  
 195 likely that *Schindleria* is completing its life cycle (i.e., one generation time) within a single  
 196 lunar cycle. Lastly, despite similar age, we found differences in the sizes and shapes of the  
 197 otoliths (Fig. 2), which may be indicative of the presence of different species among our  
 198 samples (Whittle 2003).

199

200 **Table 2:** Otolith data from 44 adult specimens of *Schindleria* from the Red Sea, collected  
 201 from May to July 2015 at three reefs along a cross-shelf gradient (one inshore “IN”, one at the  
 202 mid-shelf “MS”, and one at the shelf-edge “SE”) near the coast of Thuwal, Saudi Arabia. The  
 203 last columns “L” and “R” indicate the quality assigned (C1-C3) to each, left and right sagittal  
 204 otolith, respectively, where C1 represents poor/unreadable conditions, C2 conditions  
 205 sufficiently good for readings, and C3 ideal conditions.

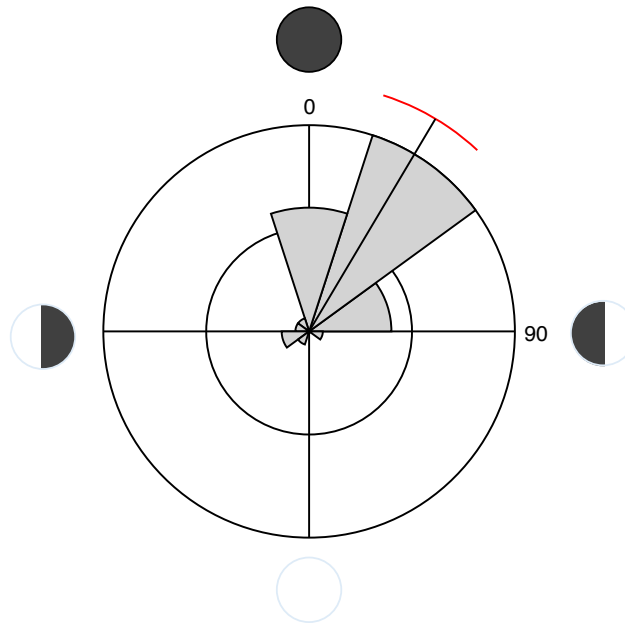
N	Reef	Age	Sampling date	Hatch date	L	R
1	IN	-	28-05-2020	-	C3	-
2	IN	36	28-05-2020	22-04-2020	-	C1
3	IN	33	28-05-2020	25-04-2020	C3	C1
4	IN	34	28-05-2020	24-04-2020	C1	C1
5	IN	30	28-05-2020	28-04-2020	C1	C3
6	IN	36	28-05-2020	22-04-2020	C2	C3
7	IN	35	28-05-2020	23-04-2020	C2	C2
8	IN	42	28-05-2020	16-04-2020	C2	C2
9	SE	31	28-05-2020	27-04-2020	C2	C3

10	SE	-	28-05-2020	-	-	-
11	SE	29	28-05-2020	29-04-2020	-	C2
12	SE	31	28-05-2020	27-04-2020	C2	C3
13	SE	32	28-05-2020	26-04-2020	C3	C3
14	SE	30	28-05-2020	28-04-2020	C3	-
15	SE	32	28-05-2020	26-04-2020	C2	C2
16	SE	36	28-05-2020	22-04-2020	C2	C1
17	MS	34	28-05-2020	24-04-2020	C3	C2
18	MS	29	28-05-2020	29-04-2020	C3	C2
19	MS	33	28-05-2020	25-04-2020	C2	C1
20	MS	34	28-05-2020	24-04-2020	C3	C2
21	MS	29	28-05-2020	29-04-2020	C2	-
22	MS	33	28-05-2020	25-04-2020	-	C2
23	MS	29	28-05-2020	29-04-2020	C2	C2
24	MS	36	28-05-2020	22-04-2020	C2	C2
25	MS	19	28-05-2020	09-05-2020	C2	C2
26	MS	33	28-05-2020	25-04-2020	C2	C2
27	MS	29	28-05-2020	29-04-2020	-	C2
28	MS	44	28-05-2020	14-04-2020	C2	C1
29	MS	37	28-05-2020	21-04-2020	C2	C2
30	MS	27	28-05-2020	01-05-2020	C2	C2
31	MS	30	28-05-2020	28-04-2020	-	C1
32	MS	39	28-05-2020	19-04-2020	C2	C2
33	IN	16	28-05-2020	12-05-2020	C2	C2
34	IN	31	28-05-2020	27-04-2020	C2	-
35	IN	33	28-05-2020	25-04-2020	C2	C2
36	MS	32	28-05-2020	26-04-2020	C3	C2
37	MS	33	28-05-2020	25-04-2020	-	C1
38	MS	33	28-05-2020	25-04-2020	C3	C2
39	MS	30	28-05-2020	28-04-2020	C1	C2
40	MS	36	28-05-2020	22-04-2020	C2	C2
41	SE	31	28-05-2020	27-04-2020	C1	C3
42	SE	33	28-05-2020	25-04-2020	C3	-
43	SE	31	28-05-2020	27-04-2020	C2	C2
44	SE	-	28-05-2020	-	-	C2

---

206

207



208

209 **Fig. 4:** Distribution of hatch frequencies of *Schindleria* from the Red Sea along a lunar cycle  
 210 (indicated with the four different black and white pie charts). The new moon corresponds to 0  
 211 ° (top), the 1<sup>st</sup> quarter moon to 90 ° (right), the full moon to 180 ° (bottom), and the 3<sup>rd</sup> quarter  
 212 moon to 270 ° (left). The “black” line gives the angular mean and the “red” arc the angular  
 213 variance of the data and the pie sections within the circle, the number of hatch events during  
 214 those lunar days.

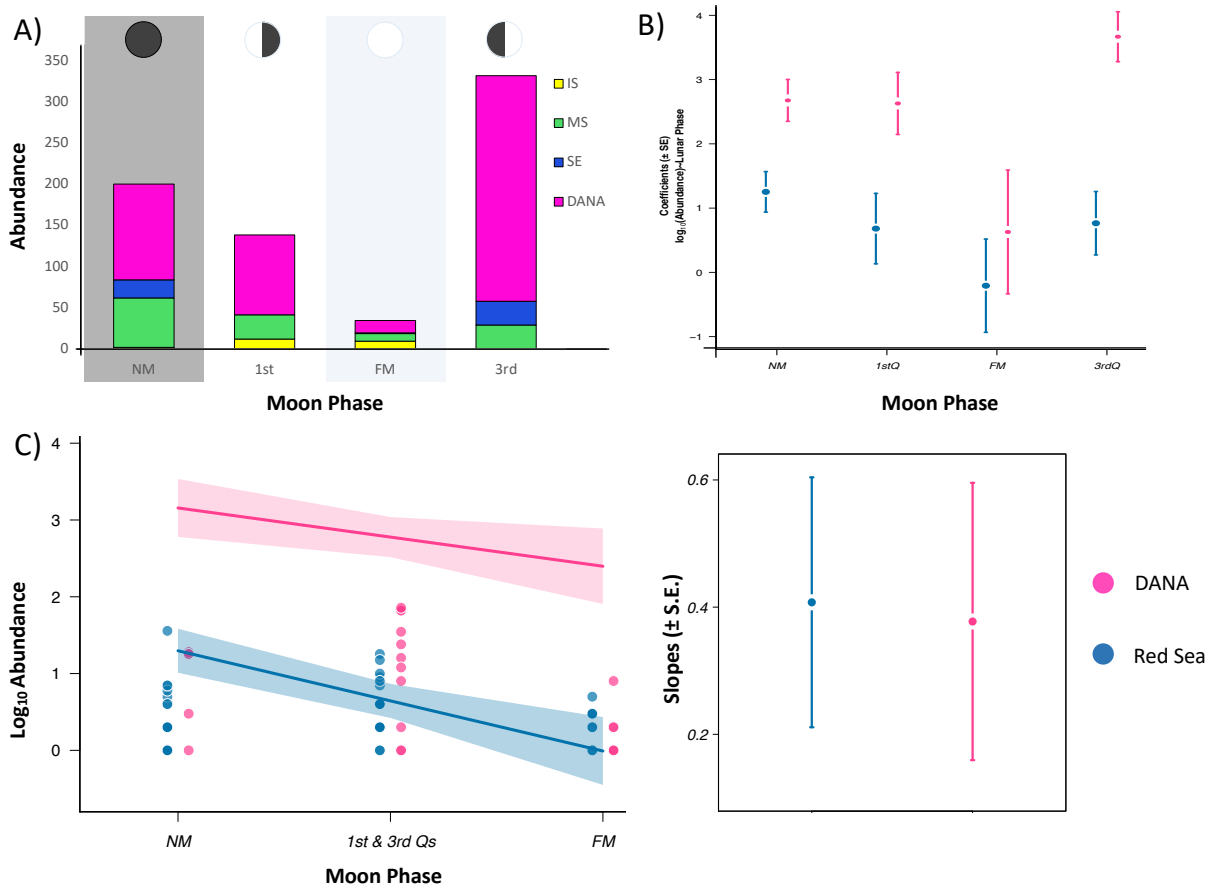
215

216 From the linear regression models, the differences in the abundances of *Schindleria* in relation  
 217 to the moon phases were most significant for the collections from the DANA Expedition, with  
 218 the highest abundances caught in the 3<sup>rd</sup> quarter moon followed by the new moon; while in the  
 219 Red Sea, it was the new moon, which yielded the highest abundances followed by the 3<sup>rd</sup> quarter  
 220 moon (see Fig. 5A and Fig. 5B). However, in both datasets, the full moon yielded the lowest  
 221 abundances, followed by the 1<sup>st</sup> quarter moon; and the differences between the full moon and  
 222 the new moon abundances were always (i.e., in the linear regressions of both datasets)  
 223 significant (Fig. 5A and Fig. 5B). Additionally, the global trend of relations between lunar  
 224 phases and abundances of *Schindleria* was supported by the slope of the generalized linear

225 models of both datasets, which were similar and of which the means did not significantly differ

226 (Fig. 5C)

227



228

229 **Fig. 5:** Relations between abundances of *Schindleria* and the four main moon phases (the new

230 moon “NM”, the 1<sup>st</sup> quarter “1stQ”, the full moon “FM”, and the 3<sup>rd</sup> quarter “3rdQ”) in two

231 different datasets: one from an Indo-Pacific collection from the DANA Expedition 1928-1930

232 (DANA) and the other from a Red Sea collection (from the 16<sup>th</sup> Oct to the 16<sup>th</sup> Nov, 2014).

233 Values from the DANA Expedition are always color-coded in “pink”. Panel A displays the

234 abundances in the Red Sea color-coded per sampling site: inshore/IS reef in “yellow”, mid-

235 shelf/MS reef in “green”, and shelf-edge/SE reef in “blue”. In Panel B and C, the Red Sea

236 abundances are given as total values in “blue”. Panel A displays the total abundances (y-axis)

237 for each dataset per moon phase (x-axis). The moon phases are represented by the circles on

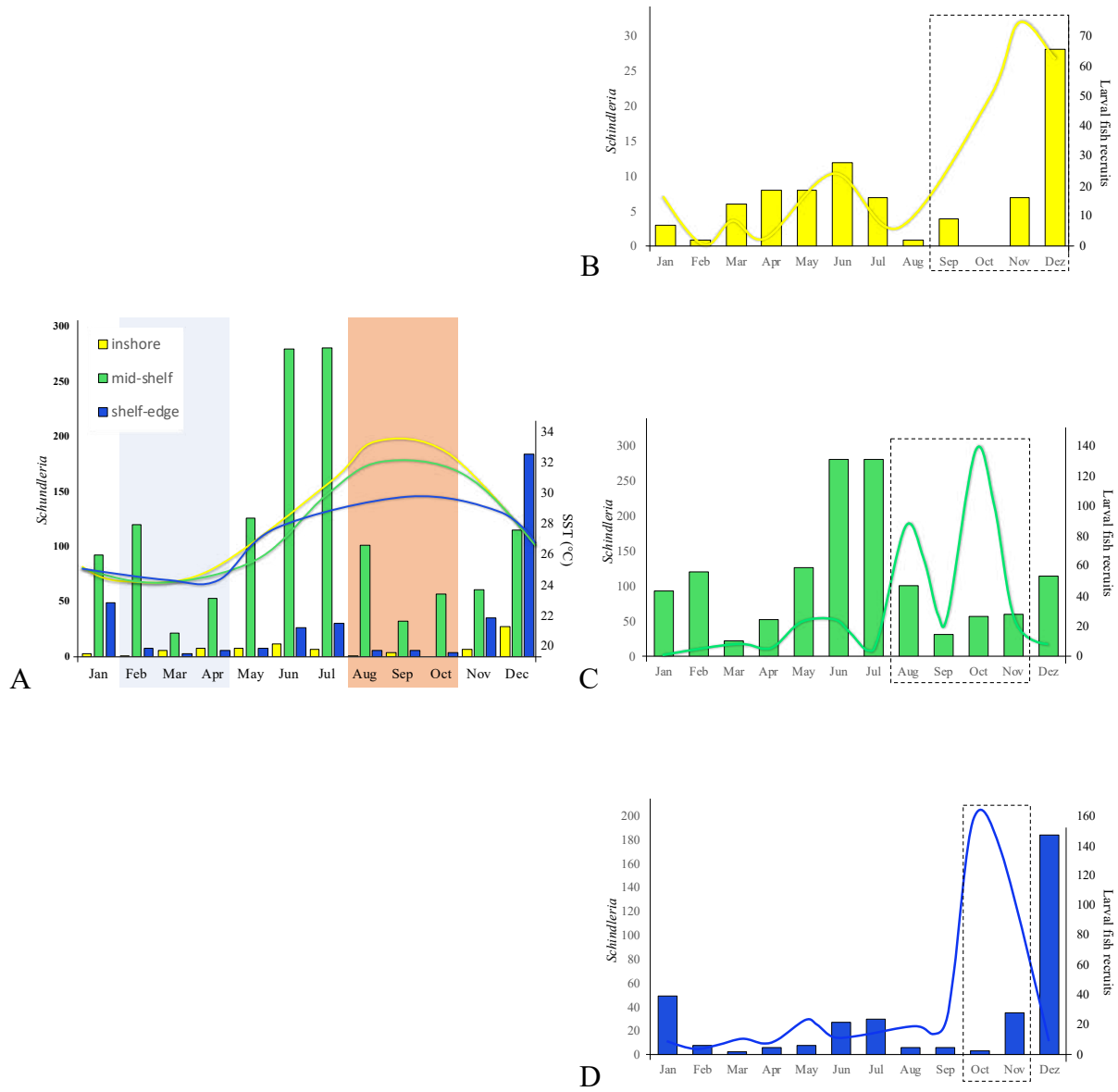
238 the top of the barplot and the brightest moon phase (FM) highlighted by a “light-blue” shaded  
239 box, while the darkest moon phase (NM) by a “black” shaded box. Panel B displays the  
240 coefficients of linear regression on the corrected  $\text{Log}_{10}$  Abundances ( $\pm$  SE; y-axis) of each moon  
241 phase (x-axis) of the two main datasets (DANA vs. Red Sea). Panel C displays, on the left plot,  
242 the abundances of each day of sampling (as dots) within a moon phase (on the x-axis; where  
243 the moon phases are grouped by light intensity for which the 1stQ and the 3rdQ moons are  
244 grouped in the middle of the regression) and on the right plot the respective slopes of the linear  
245 regression of both datasets of which the mean does not differ significantly between the two data  
246 sets. The lowest abundances of *Schindleria* were generally during the FM.

247

#### 248 *Spatio-temporal abundances of adult Schindleria within the Red Sea*

249 The mid-shelf reef site near the coast of Thuwal, Saudi Arabia, had the highest abundances of  
250 *Schindleria* among all our Red Sea sites. Seventy-five percent (1341 specimens) of the total  
251 catches were collected at this site, followed by 366 specimens collected at the shelf-edge reef,  
252 and only 85 at the inshore reef (Fig. 6). Plotting the year-round abundances of *Schindleria* for  
253 all sites and their respective sea surface temperature (SST), it was evident that the highest  
254 abundances of *Schindleria* were neither during the hottest season of the year, nor during the  
255 coolest, but rather in between those two seasonal temperature extremes (Fig. 6A). Additionally,  
256 in relation to the presence of larval fish recruits, peaks in abundances of adult *Schindleria* were  
257 also temporally decoupled from the peaks of abundances in coral reef fish recruitment (Fig. 6B-  
258 C).

259



260

261 **Fig. 6:** Barplot of the year-round abundances of adult *Schindleria* (y-axis) from the Red Sea  
 262 (Thuwal, Saudi Arabia) caught with LED powered light traps (from February 2015 to January  
 263 2016) at three different reefs along a cross-shelf gradient: one inshore (“yellow”), one at the  
 264 mid-shelf (“green”), and one at the shelf edge (“blue”). Panel A: *Schindleria* abundances in  
 265 relation to sea surface temperatures (SST, in °C). The total number of individuals for each  
 266 sampling site collected each month is given as vertical bars (values correspond to the y-axis to  
 267 the left). Temperature (SST) profiles per reef are also color-coded and given as a continuous  
 268 line (values correspond to y-axis to the right). A “light-blue” shaded box indicates the months

269 with temperature minima (February to April) and an “orange” shaded box indicates the months  
270 with temperature maxima (August to October). Peaks of abundances are observed outside both  
271 boxes. Panel B to D: *Schindleria* abundances in relation to the abundance of larval fish recruits,  
272 color-coded per reef site as in Panel A. The total number of *Schindleria* individuals collected  
273 at each sampling site is given by vertical lines and their values correspond to the left y-axis.  
274 Profiles of the abundances of larval fish recruits are given by continuous lines and their scale is  
275 given by the right y-axis. Dashed boxes indicate the months with peaks in recruitment of coral  
276 reef fish larvae (*sensu* Robitzch et al. 2020). Peaks of abundances of *Schindleria* do not  
277 generally coincide with peaks of larval fish recruitments.

278

279 Linear regression models were used to corroborate these observations. Initial models of the  
280 abundances of *Schindleria* were created for the entire data set (i.e., SST, number of larval fish  
281 recruits, reef site, and month as explanatory variables). However, the best fitting model only  
282 included the reef site as the most significant explanatory parameter, having a relative  
283 importance of 0.62 among all variables of the initial model (which explained 65.2 % of the total  
284 variance). Hence, linear regression models on the abundance of *Schindleria* were also  
285 performed per reef site. At the inshore reef, the initial model, including SST and the number of  
286 larval fish recruits, was the best fitting model and was able to explain 43.9 % of the total  
287 variance of the data with a relative importance of 0.77 for SST, and of 0.24 for the number of  
288 larval coral reef fish recruits. Contrastingly, the same initial model did not fit well neither at the  
289 mid-shelf reef nor at shelf-edge reef. In both latter cases, only very little of the variance was  
290 explained by this model (14.8 % and 2.9 %, respectively) and the number of larval fish recruits  
291 was relatively more important (0.67 - 0.99) compared to SST (0.001 - 0.33).

292

## 293 **Discussion**

294 *Schindleria*, the smallest coral reef fish in the world, potentially has the largest populations of  
295 any reef associated fish. With high turnover rates, these populations may have a substantial  
296 ecological role in reef ecosystems. Unfortunately, due to its cryptic biology and very few  
297 available studies, little is known about its basic biology and population dynamics. Putative  
298 migrations with lunar cycles may also represent an important carbon route from the pelagic into  
299 the trophic niches of the highly populated and oligotrophic coral reef matrix. We used a large  
300 collection of *Schindleria* specimens from the Red Sea (nearly two thousand specimens) and  
301 data from a recently published collection of more than 500 adult *Schindleria* from the DANA  
302 Expedition in 1928-1930<sup>8</sup> in order to access more information on the biology and reproductive  
303 behavior of this fish.

304 Even though over half of named *Schindleria* species have been described from the Red Sea,  
305 further research on the biology and ecology of this taxon is still missing, and prior to our study,  
306 only 44 adult specimens had so far been collected and documented in the Red Sea (El-Regal  
307 *pers. comm.*). In our study, we found evidence for seasonal and spatial differences in  
308 abundances likely related to differing habitat and environmental conditions among the sampled  
309 reef sites, and we also found global trends related to lunar cycles likely linked to reproductive  
310 cycles. We hypothesized that *Schindleria* would be most abundant during environmentally  
311 moderate conditions (i.e., not the hottest seasons in the Red Sea, nor those with peaks in coral  
312 reef fish recruitment) and at the darker moon phases, since these tiny pedomorphic fishes will  
313 prefer to emerge and/or approach the reef matrix in the absence of light (from the moon) to  
314 protect themselves from nocturnal visual predators; and that the collection of primarily mature  
315 specimens at the reefs may indicate trends in reproductive behavior. Back-calculations of hatch  
316 dates from the Red Sea based on otolith microincrements corroborated that *Schindleria* larvae

317 hatched a couple of days after their abundance peak during the new moon. Hence, our results  
318 supported our hypotheses of reproductive cycles of *Schindleria* being linked to the moon phases  
319 and the completion of one generation time occurring in a single lunar cycle; in addition,  
320 *Schindleria* appear to have greater success/abundances during more suitable environmental  
321 conditions. In the following we will discuss in detail our two major findings: The global trend  
322 of low abundances of *Schindleria* around the full moon and the generally high year-round  
323 abundances of *Schindleria*, yet decreased during seasonal temperature extremes and  
324 recruitment peaks of larval coral reef fishes in the Red Sea.

325

326 The Red Sea collection and that from the DANA Expedition had significant differences in the  
327 abundance of *Schindleria* in relation to moon phases. *Schindleria* was mostly absent in catches  
328 during the full moon, while peaks of abundances were during the 3<sup>rd</sup> quarter (i.e., collections  
329 from DANA Expedition) and the new moon (i.e., Red Sea collections), with a tenfold increase  
330 compared to full moon catches, in both collections.

331 In the Red Sea, the specimens caught were all mature and females carried large eggs. Hence,  
332 we suggested that high abundances during the darker moon phases may serve to reduce  
333 predation but may also be related to reproductive cycles. *Schindleria* are thought to be lagoon  
334 completers that live within the coral reef matrix<sup>11</sup>. However, recent studies have found evidence  
335 for the presence of a substantial number of adult *Schindleria* specimens far away from coral  
336 reefs (between 320 km to 360 km) in the tropical Indo-Pacific or in deeper pelagic waters (up  
337 to 1000 m depth) close to or in between coral reefs<sup>8</sup>. Hence, *Schindleria* may not be staying for  
338 their entire life-cycle within the reef matrix and may be timing their association to reefs with  
339 lunar cycles. For instance, Isari et al.<sup>24</sup> found *Schindleria* within plankton tows taken in pelagic  
340 waters close to our Red Sea sampling sites (a couple of km away from the reef). The authors

341 mainly sampled in the days prior or around the full moon, had two differing sampling sites  
342 (inshore vs. offshore), where oblique tows sampled substantially different depths (50 m depths  
343 inshore vs. 500 m depth offshore), and did not provide information on the abundances of  
344 *Schindleria* among the sampling sites, dates, or depths. However, overall, the study mainly  
345 collected juvenile *Schindleria* (S. Isari, pers. comm.), which may indicate that the abundances,  
346 distribution, and habitat or location of *Schindleria* also differs with ontogeny and that their  
347 presence at the reef matrix may be periodic, induced by seasonality of the region and lunar  
348 cycles.

349 *Schindleria* are very short-lived (max. age of 42 to 60 days<sup>1,5</sup>) and reach maturity at an  
350 extraordinarily early age for a vertebrate (23 days<sup>1</sup>). Hence, we speculated that the specimens  
351 may be reaching maturity at a certain moon phase at which they aggregate at the reefs to  
352 reproduce and spawn after which the eggs hatch (within a couple of days), larvae disperse, and  
353 the new cycle ends again with the return of the adults to the reef at the next new moon. In order  
354 to corroborate this hypothesis, we assessed the age of specimens collected at our Red Sea reef  
355 sites counting daily increments in their sagittal otoliths. Their average age was approximately  
356 33 ( $\pm$  3) days, which is close to the total length of a lunar cycle (29 days). More interestingly,  
357 the back-calculation of hatching dates for these Red Sea specimens were significantly occurring  
358 around the same lunar days and shortly after the new moon, thus supporting our hypothesis of  
359 a potential recurring reproductive aggregation during this moon phase. Hence, it may be that  
360 these specimens have generation times as short as one lunar cycle. It remains unclear why  
361 *Schindleria* evolved such a short generation time<sup>25</sup>, but our results suggest that coupling with a  
362 lunar cycle may be a strategy that works on a global scale.

363 We observed a slight shift in lunar phase with the highest abundance of *Schindleria* between  
364 the two collections studied (i.e., 3<sup>rd</sup> quarter moon in the DANA Expedition vs. the new moon

365 in the Red Sea). This could be explained by the method, the exact location of the sampling, and  
366 following the previous line of thought. The DANA specimens were not collected directly in the  
367 reef matrix (as our Red Sea specimens were) but from more pelagic waters, and the sampling  
368 method used during the DANA Expedition were plankton tows, which do not actively attract  
369 specimens within the reef-matrix (as do the light traps used during the Red Sea sampling) but  
370 capture those specimens present in the water column. Hence, while we were able to collect only  
371 mature specimens that were already at the reef to reproduce, the DANA Expedition may have  
372 collected adult specimens that were yet in the pelagic, on their way to the reef, but still a couple  
373 of days away from reaching complete maturity. The observations from inshore in the Red Sea  
374 were completely different, showing peak abundances during unexpected moon phases (the 1<sup>st</sup>  
375 quarter and the full moon). However, this site had an extremely low overall abundance of  
376 *Schindleria*, limiting the value in interpretation of these trends. Due to the small sample size, it  
377 is difficult to assess whether these reflect biological patterns or variations due to other factors  
378 (such as light intensity of the surroundings vs. the light trap, wave action, turbidity, and other  
379 factors). For example, the inshore sampling site is very close to the coastal town of Thuwal and  
380 the King Abdullah University of Science and Technology, which are both sources of noise and  
381 light at night. Sound has proven to be negatively related to the abundance of *Schindleria*  
382 (Whittle 2003). Specimens from the inshore site could have been affected by stronger coastal  
383 lights more than sites further from shore, particularly during the darker new moon. Likewise,  
384 predation risk may be increased inshore due to the stronger illumination<sup>26</sup>.

385 Overall, we were able to support our hypothesis of the alignment of a generation time and  
386 reproductive cycles with the lunar cycles in the Red Sea using data on abundances and ages of  
387 the specimens from daily microincrements from otoliths. The same support was found among  
388 abundance data of *Schindleria* from the DANA Expedition, which comprised a much wider

389 temporal and geographic range. Due to the preservation method used in the DANA collection  
390 (i.e., the samples had initially been placed in a formalin/ethanol mixture), the otolith structures  
391 were dissolved, precluding the estimation of age. Nonetheless, we hypothesize that the trends  
392 at other geographic locations will likely resemble results from the Red Sea. Other recent  
393 collection efforts using light traps at the shores of Rapa Nui/Easter Island, Chile, and in the  
394 Western Indian Ocean, also indicate higher presence of *Schindleria* during the new moon (V.  
395 Robitzch, unpubl. data).

396

397 Lastly, among the sampling sites within the Red Sea, we further concluded that the highest  
398 abundances of adult *Schindleria* were neither found during seasonal temperature extremes (i.e.,  
399 maxima and minima) nor during the peaks of coral reef fish recruitment. Most specimens were  
400 caught outside of the hottest season, which can be related to the extraordinarily high sea surface  
401 temperatures of the Red Sea<sup>24,27,28</sup> and may not hold true outside the Red Sea. However,  
402 *Schindleria*'s peaks in abundance, although outside the seasons with highest temperatures, did  
403 not coincide with the peaks of abundance of recruiting coral reef fishes in the Red Sea, which  
404 is also outside of the hottest season<sup>24,27</sup>. We explain the difference in peaks with the longevity  
405 and biology of *Schindleria*. As opposed to longer-lived coral reef fishes, *Schindleria* cannot  
406 time reproduction or the termination of their PLD in the long term; the species' longevity  
407 demands monthly, year-round reproduction<sup>29,30</sup>. Nonetheless, its larvae are likely benefitting  
408 from the same conditions as are other coral fish larvae<sup>27</sup>. Hence, *Schindleria* may have a more  
409 successful PLD outside the periods of peaks in coral reef fish reproduction, since it will likely  
410 have less competition for resources, particularly within the extremely oligotrophic central Red  
411 Sea. The mortality of premature phases of *Schindleria* may also increase during abundance  
412 peaks of coral reef fish larvae as these may prey on tiny *Schindleria* leaving fewer adults that

413 survive the PLD. Due to the morphological similarity between adult *Schindleria* and fish larvae,  
414 both may have similar predators. Hence, the abundance of *Schindleria* may be seasonally  
415 reduced during periods of recruitment peaks of coral reef fish larvae because of associated  
416 higher abundances of predators adapted to feed on incoming larval recruiting cohorts.  
417 Nevertheless, we argue that *Schindleria*'s unique life history and short generation time forces  
418 it to start a new generation every month "despite the weather", which is why it is generally  
419 abundant year-round. The longevity and biology of *Schindleria* may also further explain why  
420 its behavioral cycles follow lunar cycles globally as environmental conditions become less  
421 important when periodicity needs to be established and a generation must be completed within  
422 a few weeks. Schindleriidae is yet a species-poor monogeneric family, likely due to the lack of  
423 data rather than the lack of biodiversity; and a large number of cryptic species are likely to be  
424 found within this taxon<sup>7</sup>. Hence, species-specific trends are yet far from understood and the  
425 differences in otoliths structures we found suggest the presence of several species at small  
426 scales<sup>26</sup>. With increased research on the species' diversity of this taxon, further discoveries of  
427 discrepancies and preferences in *Schindleria*'s ecology, biology, recurring cyclic behavior, and  
428 habitats will rise. Accordingly, some of the differences in the spatial yearlong abundances as  
429 well as in the site-specific temporal abundances we found in adult *Schindleria* may further be  
430 distinctive among species and their specific biological and ecological features.

431

## 432 **Methods**

### 433 *Sampling and data*

434 *Schindleria* samples were collected at three reefs: one reef inshore "IS", one at the mid-shelf  
435 "MS", and one at the shelf-edge "SE" off of the coast of Thuwal, Red Sea, Saudi Arabia (blue,  
436 green, and yellow reef, respectively, in the zoomed map section of Fig. 1), using a set of three

437 replicate light traps per reef (i.e., nine light traps total) attached to fixed moorings positioning  
438 the light trap ~2 m below the surface, at the northern end of the wave-protected (eastern) side  
439 of each reef, with a bottom depth of approx. 8 m to 14 m. Prior to each sampling night, the  
440 rechargeable batteries of the light traps were replaced with fully charged ones and each light  
441 trap and mooring were cleaned to assure the same starting conditions for each sampling period  
442 and to avoid sampling biases due to algal growth, reduced light intensity, or induced chemical  
443 cues. For all qualitative and quantitative analyses, the daily catches from all three light traps  
444 were pooled for each reef. This research was undertaken in accordance with the policies and  
445 procedures of the King Abdullah University of Science and Technology (KAUST). Permits for  
446 sampling in Saudi Arabian waters were obtained from the relevant Saudi Arabian authorities.  
447 The study did not involve live specimens or endangered or protected species. KAUST  
448 implemented its Institutional Animal Care and Use Committee in December 2016; the  
449 collections in this paper were concluded prior to that date.

450

#### 451 *Correlations of abundances of Schindleria with lunar phases*

452 The collapsible LED light traps (Bellamare 500-micron mesh) were first deployed for 32  
453 consecutive days (from the 16<sup>th</sup> October to the 16<sup>th</sup> November 2014) to capture variation in  
454 abundance related to lunar phases (within a complete lunar month). The daily light trap samples  
455 were assigned to one of four main moon phases depending on the date of their collection relative  
456 to the lunar day: the new moon “NM” (comprising the 26<sup>th</sup>-29<sup>th</sup> and the 1<sup>st</sup>-4<sup>th</sup> lunar day), the  
457 1<sup>st</sup> quarter “1stQ” (from the 5<sup>th</sup>-11<sup>th</sup> lunar day), the full moon “FM” (from the 12<sup>th</sup>-19<sup>th</sup> lunar  
458 day), and the 3<sup>rd</sup> quarter “3rdQ” (from the 20<sup>th</sup>-25<sup>th</sup> lunar day).

459 To further assess the importance of moon phases on the abundance of *Schindleria* on a global  
460 scale, data on *Schindleria* abundances from sampling stations from the DANA Expedition

461 1928-1930 (i.e., all sampling points outside the Red Sea (ID1 – ID44)<sup>8</sup> in Fig. 1) were taken  
462 and categorized into the four main moon phases in the same way as the Red Sea data. The  
463 “moon phase” was then used as the explanatory variable (i.e., as a factor) for the abundance of  
464 *Schindleria* from the DANA Expedition and from the Red Sea in two separate linear regression  
465 models (generalized linear models in R, *glm* function, R Core Team<sup>31</sup>). The linear regression  
466 models were then compared to one another. Due to overdispersion observed in both data sets  
467 (evaluated by using the dispersion test in the *AER* R package<sup>32,33</sup>) we used the quasi-poisson  
468 family distribution in the *glm* function to fit the model. An ANOVA was then performed  
469 between the null-model and our alternative model. To compare the results of the glms of both  
470 data sets, we plotted the  $\log_{10}$  coefficients of the linear regressions of the abundances in the  
471 different moon phases of both datasets in order to assess the significance of the differences of  
472 abundances of *Schindleria* among the different moon phases, and whether these changes in  
473 abundances were similar between the two data sets. In this regard, to compare the slopes of the  
474 linear regression models of the two datasets, the moon phases were converted to numeric ranks  
475 following the light intensity of each moon phase for which the “NM” was given the value “0”,  
476 the FM the value “2” and the 1<sup>st</sup> and 3<sup>rd</sup> quarter moons (1stQ and 3rdQ) the value of “1”, since  
477 both of them represent the value of one illuminated quarter of the moon. The *glm* function was  
478 then again applied using the quasi-poisson family to correct for overdispersion of the data; and  
479 the respective slopes of the models of each dataset (Red Sea vs. DANA) were plotted to check  
480 for significant differences in the correlations between moon phases and abundances of  
481 *Schindleria*.

482         As a last step to examine potential relations of *Schindleria* catches with moon phases,  
483 the age of mature *Schindleria* specimens (i.e., females with visibly developed oocytes and  
484 males with distinctive urogenital papillae) collected in the three Red Sea locations (preserved

485 in 95% EtOH) were assessed by counting daily growth increments of the sagittal otoliths. Right  
486 and left sagittal otoliths were removed under an Olympus SZ61 stereomicroscope equipped  
487 with a polarized light filter. The pair of otoliths was completely immersed in epoxy resin and  
488 fixed to a microscopy slide. The otoliths were then photographed under a Zeiss AXIO Lab.A1A  
489 microscope equipped with an ATRAY camera. No further preparation was needed to reveal  
490 daily increments. Additionally, the pictures taken from the otoliths for the counts of  
491 microincrements were categorized with a qualitative scale (C1 – C3), where C1 had poor  
492 resolution, were too damaged and/or in a state that made the readings of microincrements  
493 impossible, and were thus discarded from the analysis; C2 had tissue remains or were broken  
494 but provided enough resolution to assess numbers of microincrements; and C3 were in ideal  
495 condition. Normality of the data was then tested using the Shapiro-Wilk test. Counts of the right  
496 and/or the left sagittae were used, because both counts did not differ significantly (*Wilcoxon-*  
497 *test,  $z = 0.30, P = 0.76$* ). Therefore, in cases where one of the two sagittae otoliths were broken  
498 or too blurry to measure, the other available otolith was used. The otoliths were counted at least  
499 three times by an independent reader (Camilo Rodríguez-Valentino), who lacked any  
500 information on the samples or the study purpose in order to obtain unbiased estimates of the  
501 age of each sample and its hatch date. To assess the hatch frequencies over the lunar cycle, the  
502 hatch dates were back-calculated from the sampling date. Then, the “Lunar hatch day” (LHD)  
503 was determined to transform the lunar cycle to an angle variable. Thus, the lunar cycle (of 29  
504 days) was converted to a 360° cycle, setting the new moon as day 1. Thereby, LHD = the  
505 number of days since the new moon\*(360/29). A uniform distribution around the lunar cycle  
506 was tested using Rao’s spacing test<sup>34</sup> as it is a robust circular statistical test able to analyze bi-  
507 and multimodal distributions. All statistical analyses related to otolith increments were  
508 performed using the free software Past 4.0<sup>35</sup>.

509

510 *Relationships of abundances of Schindleria with temporal and spatial conditions*

511 After the month of daily sampling of *Schindleria*, the same light traps were deployed during  
512 five consecutive nights around the new moon for twelve consecutive months at the same  
513 moorings, to assess variation in abundance related to seasonal environmental (i.e., temporal)  
514 conditions and habitat/site-related (i.e., spatial) differences among the reefs within the Red Sea  
515 (i.e., the “IS”, the “MS”, and the “SE” reef). Hence, sea surface temperatures (SST) at each reef  
516 were further recorded during the sampling period with an acoustic doppler current profiler  
517 (ADCP, Nortek AS, data available in Appendix S3<sup>27</sup>). The light traps also attracted larval fish  
518 recruits of which the abundances were measured and were spatio-temporally regulated by  
519 environmental conditions<sup>27</sup>. We included said abundances as a predictive variable for the  
520 abundance of *Schindleria*, since the abundance of these larval coral reef fish recruits already  
521 comprised/reflected a range of ecosystem and environmental parameters/conditions and was  
522 therefore considered as a good proxy to represent changes in the environment and habitat.  
523 Additionally, physiologically and morphologically, adult *Schindleria* strongly resemble fish  
524 larvae for which the relation between the abundance of said larvae and that of mature  
525 *Schindleria* is further interesting. While adult *Schindleria* are often mistaken for a larva, their  
526 ontogeny may lead to differing ecological and biological features, which may also be reflected  
527 in their abundance. Hence, the local abundances of larval coral reef fish recruits (as total counts)  
528 together with the sampling location (as the reef site), the SST (in °C), and the month of sampling  
529 were considered in the initial model to perform linear regression on the abundances of  
530 *Schindleria*.

531

532 **References**

- 533 1. Kon, T. & Yoshino, T. Diversity and evolution of life histories of gobioid fishes from  
534 the viewpoint of heterochrony. *Mar. Freshw. Res.* **53**, 377–402 (2002).
- 535 2. Randall, J. E. & Cea, A. *Shore fishes of Easter Island*. (University of Hawaii Press,  
536 2011).
- 537 3. Kon, T., Yoshino, T., Mukai, T. & Nishida, M. DNA sequences identify numerous  
538 cryptic species of the vertebrate: a lesson from the gobioid fish *Schindleria*. *Mol.*  
539 *Phylogenet. Evol.* **44**, 53–62 (2007).
- 540 4. Johnson, G. D. & Brothers, E. B. *Schindleria*: a paedomorphic goby (Teleostei:  
541 Gobioidae). *Bull. Mar. Sci.* **52**, 441–471 (1993).
- 542 5. Landaeta, M. F., Veas, R. & Castro, L. R. First record of the paedomorphic goby  
543 *Schindleria praematura*, Easter Island, South Pacific. *J. Fish Biol.* **61**, 289–292 (2002).
- 544 6. Watson, W. & Walker, H. J. J. The world’s smallest vertebrate, *Schindleria*  
545 *brevipinguis*, a new paedomorphic species in the family Schindleriidae (Perciformes:  
546 Gobioidae). *Rec. Aust. Museum* **56**, 139–142 (2004).
- 547 7. Kon, T., Yoshino, T. & Nishida, M. Cryptic species of the gobioid paedomorphic  
548 genus *Schindleria* from Palau, Western Pacific Ocean. *Ichthyol. Res.* (2010)  
549 doi:10.1007/s10228-010-0178-y.
- 550 8. Ahnelt, H. & Sauberer, M. Deep-water, offshore, and new records of Schindler’s  
551 fishes, *Schindleria* (Teleostei, Gobiidae), from the Indo-west Pacific collected during  
552 the Dana-Expedition, 1928–1930. *Zootaxa* **4731**, 451–470 (2020).
- 553 9. Bruun, A. F. A study of a collection of the fish *Schindleria* from South Pacific waters.  
554 *Dana Rep.* **21**, 1–12 (1940).
- 555 10. Jones, S. & Kumaran, M. On the fishes of the genus *Schindleria* (Giltay) from the  
556 Indian Ocean. *J. Mar. Biol.* **6**, 257–264 (1964).
- 557 11. Leis, J. M. Coral sea atoll lagoons: closed nurseries for the larvae of a few coral reef  
558 fishes. *Bull. Mar. Sci.* **54**, 206–227 (1994).
- 559 12. Belyanina, T. P. Ichthyoplankton in the regions of the Nazca and Salas y Gomez  
560 submarine ridges. *J. Ichthyol.* **29**, 84–90 (1989).
- 561 13. Parin, N. V., Mironov, A. N. & Nesis, K. N. Biology of the Nazca and Salas y Gomez  
562 submarine ridges, an outpost of the Indo-West Pacific fauna in the Eastern Pacific  
563 Ocean: composition and distribution of the fauna, its communities and history. *Adv.*  
564 *Mar. Biol.* **32**, 147–242 (1997).
- 565 14. Ahnelt, H. & Sauberer, M. A new species of Schindler’s fish (Teleostei: Gobiidae:  
566 *Schindleria*) from the Malay archipelago (Southeast Asia), with notes on the caudal fin  
567 complex of *Schindleria*. *Zootaxa* **4531**, 95–108 (2018).
- 568 15. Thacker, C. & Grier, H. Unusual gonad structure in the paedomorphic teleost  
569 *Schindleria praematura* (Teleostei Gobioidae): a comparison with other gobioid fishes.  
570 *J. Fish Biol.* **66**, 378–391 (2005).
- 571 16. Young, S.-S. & Chiu, T.-S. New records of a paedomorphic fish *Schindleria*  
572 *praematura* (Pisces: Schindleriidae), from Waters of Taiwan. *Acta Zool. Taiwanica* **11**,  
573 127–137 (2000).
- 574 17. Watson, W. & Leis, J. M. Ichthyoplankton of Kaneohe Bay, Hawaii. A one-year study  
575 of fish eggs and larvae. *University of Hawai‘i Sea Grant Program* 1–178 (1974).
- 576 18. Fricke, R. & El-Regal, M. A. *Schindleria nigropunctata*, a new species of  
577 paedomorphic gobioid fish from the Red Sea (Teleostei: Schindleriidae). *Mar.*  
578 *Biodivers.* (2017).
- 579 19. Fricke, R. & El-Regal, M. A. *Schindleria elongata*, a new species of paedomorphic  
580 gobioid from the Red Sea (Teleostei: Schindleriidae). *J. Fish Biol.* 1–8 (2017)  
581 doi:10.1111/jfb.13280.
- 582 20. Schindler, O. Ein neuer Hemiramphus aus dem Pazifischen Ozean. *Anzeiger der*  
583 *Akad. der Wissenschaften Wien* **68**, 2–3 (1931).

- 584 21. Schindler, O. Ein neuer Hemirhamphus aus dem Pazifischen Ozean. *Anzeiger der*  
585 *Akad. der Wissenschaften Wien* **67**, 79–80 (1930).
- 586 22. Ahnelt, H. Redescription of the paedomorphic goby *Schindleria nigropunctata* Fricke  
587 & El-Regal 2017 (Teleostei: Gobiidae) from the Red Sea. *Zootaxa* **4615**, 450–456  
588 (2019).
- 589 23. Contreras, J. E., Landaeta, M. F., Plaza, G., Ojeda, F. P. & Bustos, C. A. The  
590 contrasting hatching patterns and larval growth of two sympatric clingfishes inferred by  
591 otolith microstructure analysis. *Mar. Freshw. Res.* **64**, 157–167 (2013).
- 592 24. Isari, S. *et al.* Exploring the larval fish community of the central Red Sea with an  
593 integrated morphological and molecular approach. *PLoS One* **12**, 1–24 (2017).
- 594 25. Depczynski, M. & Bellwood, D. R. Extremes, plasticity, and invariance in vertebrate  
595 life history traits: Insights from coral reef fishes. *Ecology* **87**, 3119–3127 (2006).
- 596 26. Whittle, A. G. Ecology, abundance, diversity, and distribution of larval fishes and  
597 Schindleriidae (Teleostei: Gobioidi) at two sites on O’ahu, Hawai’i. (University of  
598 Hawai’i, 2003).
- 599 27. Robitzch, V. & Berumen, M. L. Recruitment of coral reef fishes along a cross-shelf  
600 gradient in the Red Sea peaks outside the hottest season. *Coral Reefs* **39**, 1565–1579  
601 (2020).
- 602 28. Nanninga, G. B., Saenz-Agudelo, P., Zhan, P., Hoteit, I. & Berumen, M. L. Not finding  
603 Nemo: limited reef-scale retention in a coral reef fish. *Coral Reefs* **34**, 383–392 (2015).
- 604 29. Hernaman, V. & Munday, P. L. Life-history characteristics of coral reef gobies. I.  
605 Growth and life-span. *Mar. Ecol. Prog. Ser.* **290**, 207–221 (2005).
- 606 30. Lefèvre, C. D., Nash, K. L., González-Cabello, A. & Bellwood, D. R. Consequences of  
607 extreme life history traits on population persistence: do short-lived gobies face  
608 demographic bottlenecks? *Coral Reefs* **35**, 399–409 (2016).
- 609 31. Team, R. C. R: A language and environment for statistical computing (Version 3.6).  
610 <https://www.R-project.org> (2020).
- 611 32. Kleiber, C. & Zeileis, A. *Applied econometrics with R*. (Springer Science & Business  
612 Media, 2008).
- 613 33. Kleiber, C. & Zeileis, A. AER: Applied Econometrics with R. R package version 1.1.  
614 (2009).
- 615 34. Batschelet, E. *Circular statistics in biology*. (Academic Press, 1981).
- 616 35. Hammer, Ø., Harper, D. A. T., Ryan, P. D. & others. PAST: Paleontological statistics  
617 software package for education and data analysis. *Palaeontol. Electron.* **4**, 9 (2001).
- 618
- 619

620 **Author contributions:** V.R. conceived the idea and collected the samples for this study.

621 V.R., V.M-V., J.J.S-I., and M.L. analyzed and interpreted the data. V.R., V.M-V., J.J.S-I., M.L.,

622 and M.L.B discussed the results and made significant contributions leading to the final

623 construction of the manuscript.

624

625 **Competing interests’ statement:** The authors declare no competing interests.



## Figures

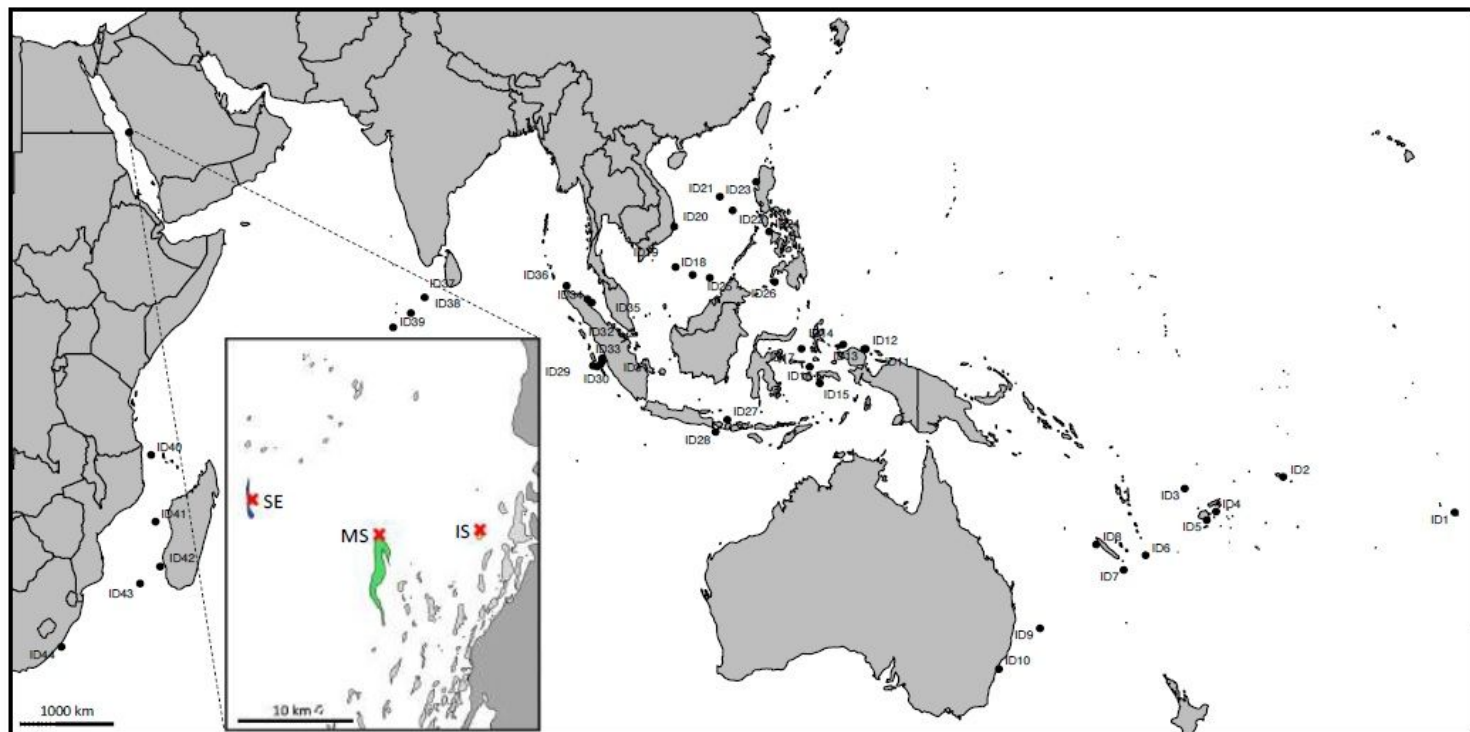


**Figure 1**

Collection sites of *Schindleria*: from the DANA Expedition 1928-1930 (all sites represented by a “dot”: ID1 – ID44, following Ahnelt and Sauberer 20208); and from the Red Sea, with a zoomed-in section displaying the three reefs where collection took place using a LED powered light trap along a cross-shelf gradient from the shore to the shelf edge, near the coast of Thuwal, Saudi Arabia. Coral reefs within the zoomed-in Red Sea section are given in “light grey” while the land sections are in “dark grey” and the sampled reef sites are color coded, with the “yellow” reef inshore (IS), the “green” reef at the mid-shelf (MS), and the “blue” reef at the shelf edge (SE). The “red” crosses indicate the location of deployment of the LED powered light traps for this study. Note: The designations employed and the presentation of the material on this map do not imply the expression of any opinion whatsoever on the part of Research Square concerning the legal status of any country, territory, city or area or of its authorities, or concerning the delimitation of its frontiers or boundaries. This map has been provided by the authors.

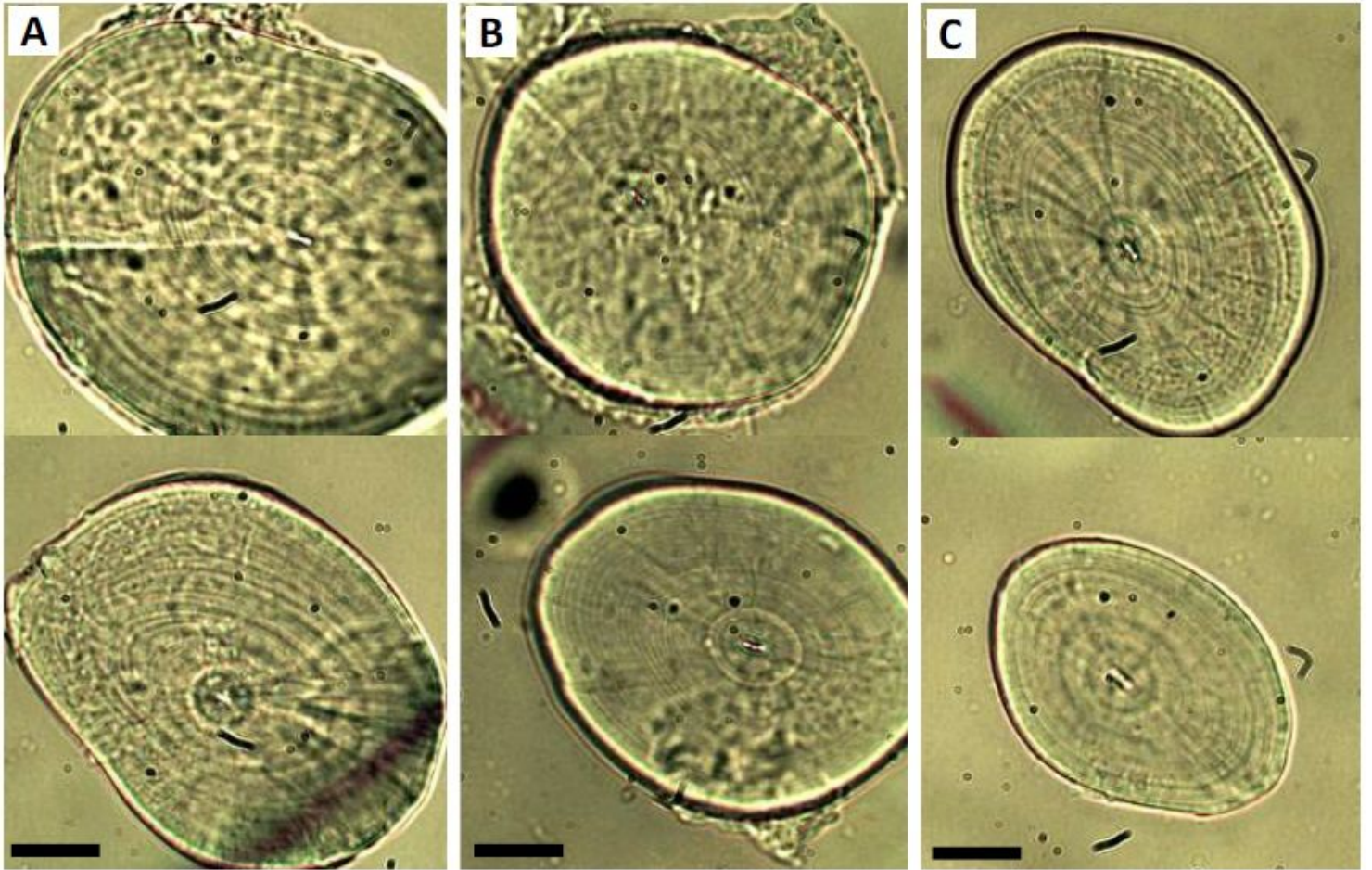


**Figure 2**

Sagittal otoliths from mature *Schindleria* specimens sampled with light traps from an inshore (A), a mid-shelf (B), and a shelf-edge (C) reef in the Red Sea, near the coast of Thuwal, Saudi Arabia. These otoliths represent otoliths of ideal conditions (i.e., “C3” category) to count daily growth increments and yielded average numbers of increments (between 30-33) despite slightly differing shapes and sizes. All otoliths are to scaled, with the bar at the bottom (left) of each panel representing 20  $\mu\text{m}$ . The otolith at the top of each panel represents a rounder and larger otolith while the otolith at the bottom a more oval-shaped and smaller otolith.

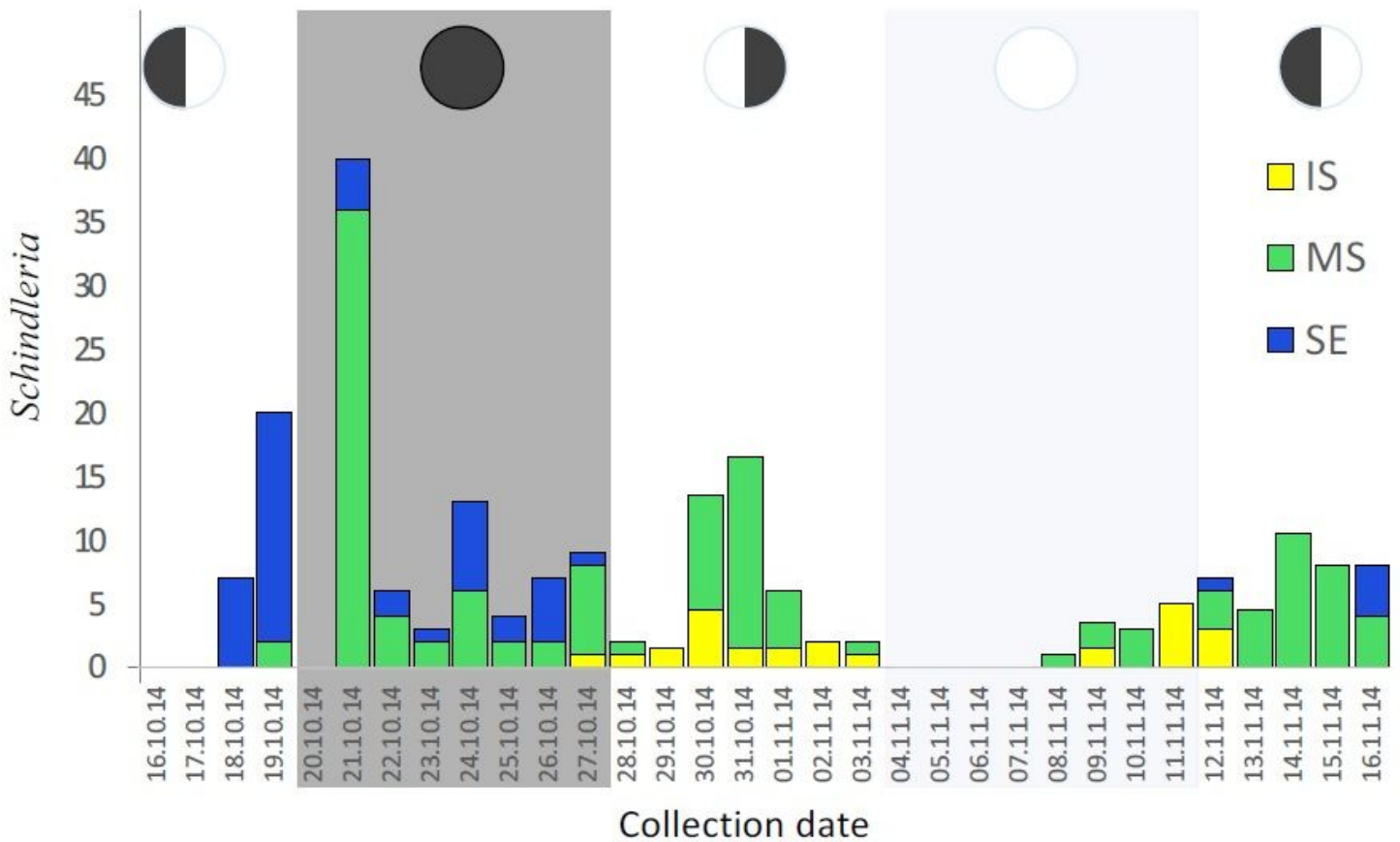


**Figure 3**

Barplot representing the total abundances of *Schindleria* collected during one lunar cycle in the Red Sea of Saudi Arabia. Total numbers of *Schindleria* specimens (y-axis) collected are color-coded for the relative number caught at each of three sampling locations: an inshore reef (IS) in “yellow”, a reef at the mid-shelf (MS) in “green”, and one at the shelf-edge (SE) in “blue”. Collections took place using three replicate LED powered light traps (collapsible Bellamare model) at each sampling location for the period of 32 consecutive nights from the 16th October to the 16th November (2014; x-axis). Different moon phases are indicated with pie charts on the top of each shaded section of the plot starting with the 3rd quarter moon, followed by the new moon, the 1st quarter moon, the full moon, and ending again with the 3rd quarter moon (from left to right).

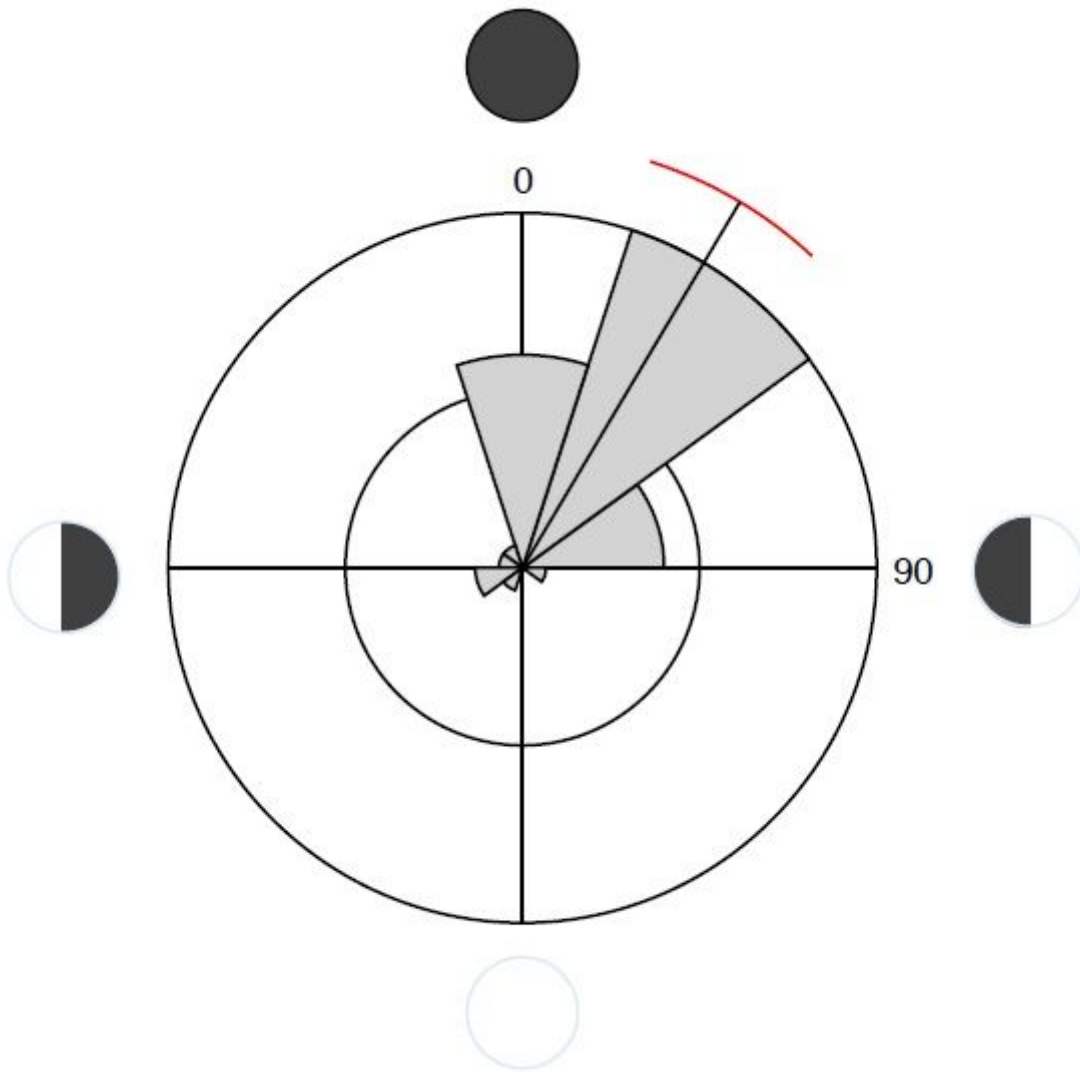


**Figure 4**

Distribution of hatch frequencies of *Schindleria* from the Red Sea along a lunar cycle (indicated with the four different black and white pie charts). The new moon corresponds to  $0^\circ$  (top), the 1st quarter moon to  $90^\circ$  (right), the full moon to  $180^\circ$  (bottom), and the 3rd quarter moon to  $270^\circ$  (left). The “black” line gives the angular mean and the “red” arc the angular variance of the data and the pie sections within the circle, the number of hatch events during those lunar days.

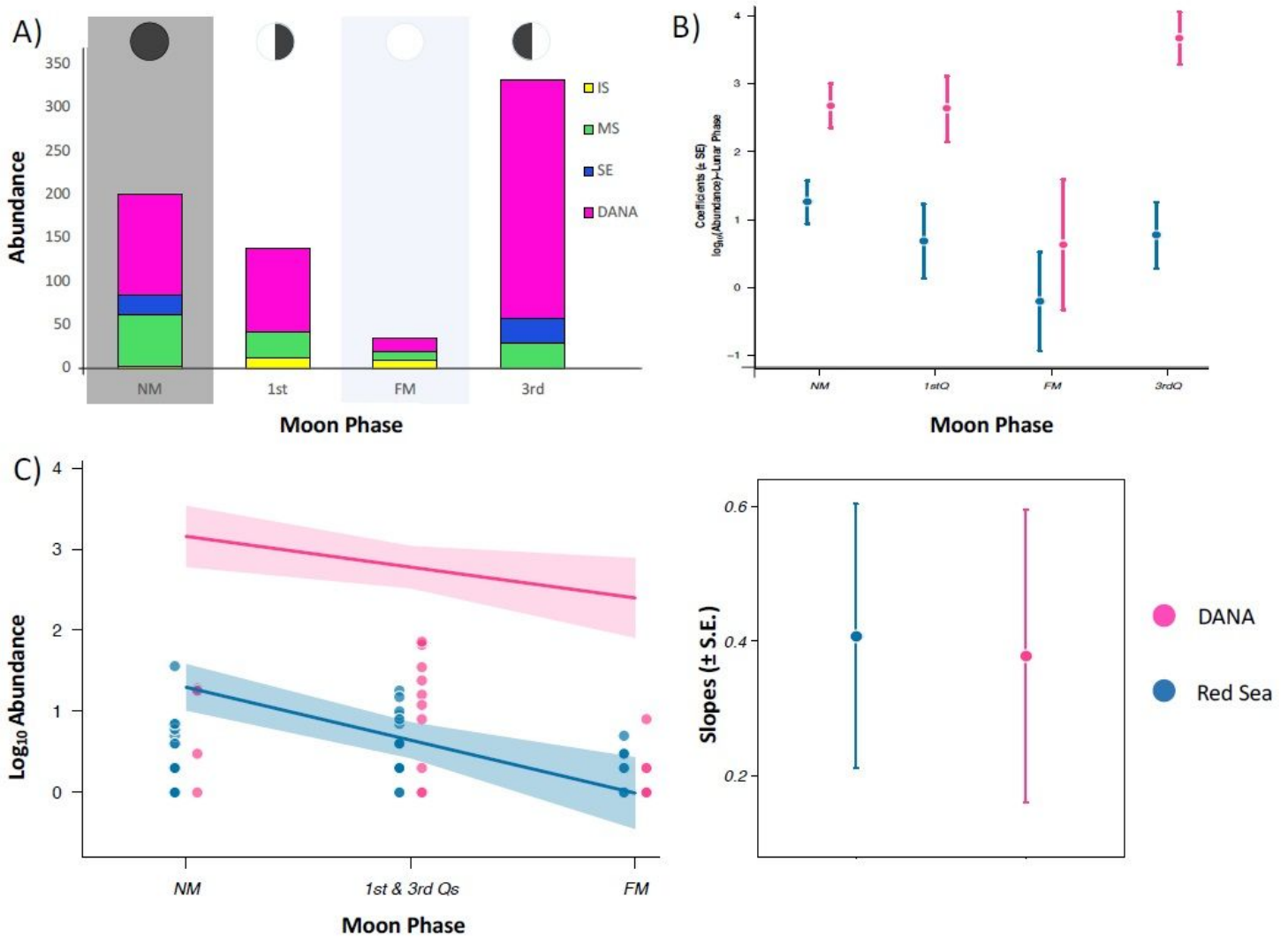


**Figure 5**

Relations between abundances of *Schindleria* and the four main moon phases (the new moon “NM”, the 1st quarter “1stQ”, the full moon “FM”, and the 3rd quarter “3rdQ”) in two different datasets: one from an Indo-Pacific collection from the DANA Expedition 1928-1930 (DANA) and the other from a Red Sea collection (from the 16th Oct to the 16th Nov, 2014). Values from the DANA Expedition are always color-coded in “pink”. Panel A displays the abundances in the Red Sea color-coded per sampling site: inshore/IS reef in “yellow”, mid shelf/MS reef in “green”, and shelf-edge/SE reef in “blue”. In Panel B and C, the Red Sea abundances are given as total values in “blue”. Panel A displays the total abundances (y-axis) for each dataset per moon phase (x-axis). The moon phases are represented by the circles on the top of the barplot and the brightest moon phase (FM) highlighted by a “light-blue” shaded box, while the darkest moon phase (NM) by a “black” shaded box. Panel B displays the coefficients of linear regression on the corrected  $\log_{10}$  Abundances ( $\pm$  SE; y-axis) of each moon phase (x-axis) of the two main datasets (DANA vs. Red Sea). Panel C displays, on the left plot, the abundances of each day of sampling (as dots) within a moon phase (on the x-axis; where the moon phases are grouped by light intensity for which the

1stQ and the 3rdQ moons are grouped in the middle of the regression) and on the right plot the respective slopes of the linear regression of both datasets of which the mean does not differ significantly between the two data sets. The lowest abundances of *Schindleria* were generally during the FM.

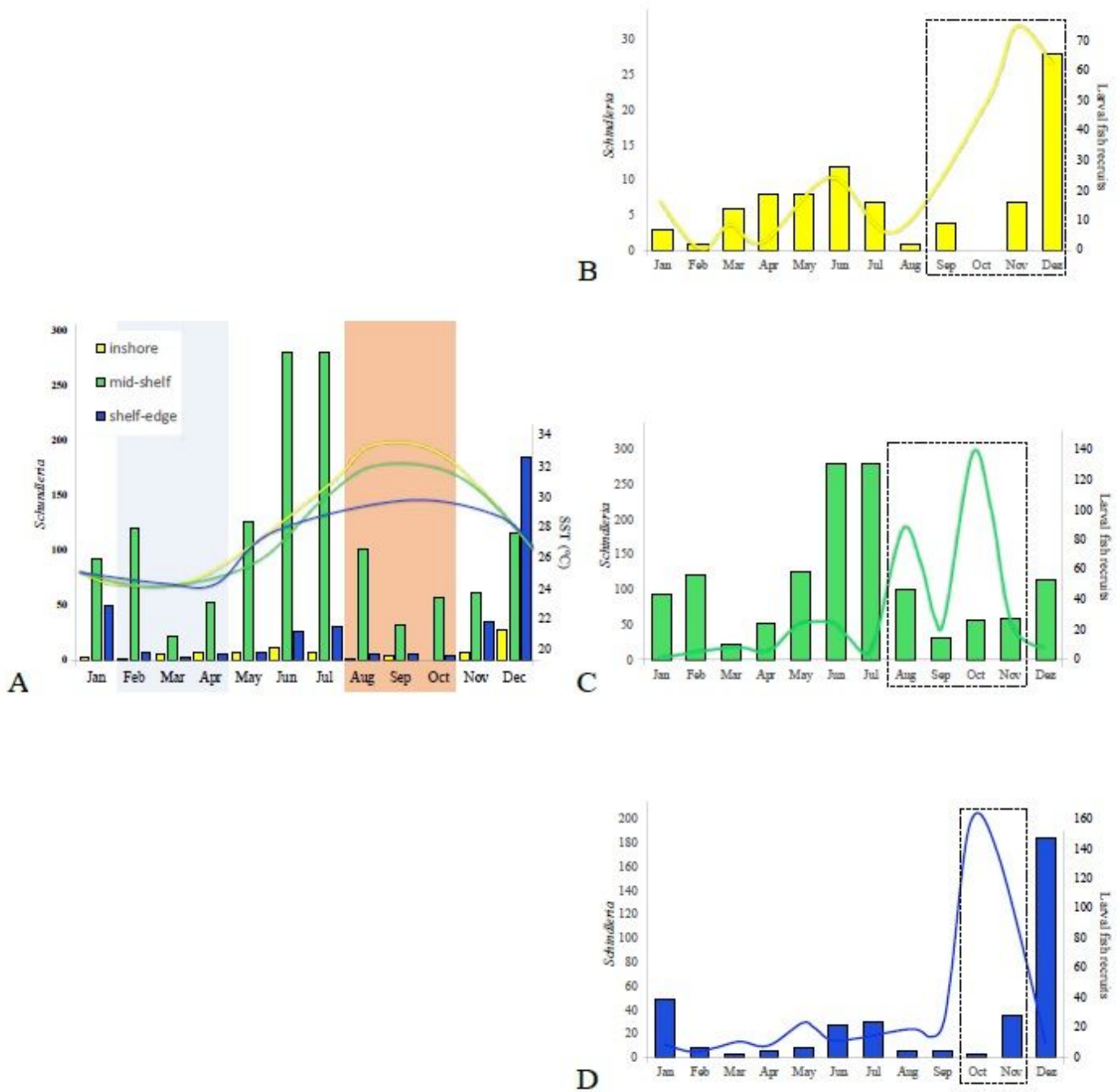


**Figure 6**

Barplot of the year-round abundances of adult *Schindleria* (y-axis) from the Red Sea (Thuwal, Saudi Arabia) caught with LED powered light traps (from February 2015 to January 2016) at three different reefs along a cross-shelf gradient: one inshore (“yellow”), one at the mid-shelf (“green”), and one at the shelf edge (“blue”). Panel A: *Schindleria* abundances in relation to sea surface temperatures (SST, in °C). The total number of individuals for each sampling site collected each month is given as vertical bars

(values correspond to the y-axis to the left). Temperature (SST) profiles per reef are also color-coded and given as a continuous line (values correspond to y-axis to the right). A “light-blue” shaded box indicates the months with temperature minima (February to April) and an “orange” shaded box indicates the months with temperature maxima (August to October). Peaks of abundances are observed outside both boxes. Panel B to D: *Schindleria* abundances in relation to the abundance of larval fish recruits, color-coded per reef site as in Panel A. The total number of *Schindleria* individuals collected at each sampling site is given by vertical lines and their values correspond to the left y-axis. Profiles of the abundances of larval fish recruits are given by continuous lines and their scale is given by the right y-axis. Dashed boxes indicate the months with peaks in recruitment of coral reef fish larvae (sensu Robitzsch et al. 2020). Peaks of abundances of *Schindleria* do not generally coincide with peaks of larval fish recruitments.